RAPID COMMUNICATIONS

PHYSICAL REVIEW B **92**, 161402(R) (2015)

Negative static permittivity and violation of Kramers-Kronig relations in quasi-two-dimensional crystals

V. U. Nazarov

Research Center for Applied Sciences, Academia Sinica, Taipei 11529, Taiwan

(Received 18 June 2015; published 6 October 2015)

We investigate the wave vector and frequency-dependent screening of the electric field in atomically thin (quasi-two-dimensional) crystals. For graphene and hexagonal boron nitride we find that, above a critical wave vector q_c, the static permittivity $\varepsilon(q > q_c,\omega = 0)$ becomes negative and the Kramers-Kronig relations do not hold for $\varepsilon(q > q_c,\omega)$. Thus, in quasi-two-dimensional crystals, we reveal the physical confirmation of a proposition put forward decades ago [D. A. Kirzhnits, Sov. Phys. Usp. **19**, 530 (1976)], allowing for the breakdown of Kramers-Kronig relations and for negative static permittivity. In the vicinity of the critical wave vector, we find a giant growth of the permittivity. Our results, obtained in the *ab initio* calculations using both the random-phase approximation and the adiabatic time-dependent local-density approximation, and further confirmed with a simple slab model, allow us to argue that the above properties, being exceptional in the three-dimensional case, are common to quasi-two-dimensional systems.

DOI: 10.1103/PhysRevB.92.161402 PACS number(s): 77.22.Ch, 73.22.Pr, 73.90.+f

The concept of causality plays one of the central roles in contemporary science [1]. It is well known that causality in the time domain (the impossibility for an effect to precede the cause in time) leads to the analyticity of a causal response function in a complex half plane in the frequency domain, which in turn leads to Kramers-Kronig (KK) relations between the real and the imaginary parts of the response function [2].

It must, however, be recognized that the causality assumes that the response function is applied to a cause and it produces an effect. In the case of a longitudinal electric field in a translationally invariant or a periodic system, the definition of the permittivity $\varepsilon(\mathbf{q},\omega)$ reads $\phi_{\text{tot}}(\mathbf{q},\omega) = \phi_{\text{ext}}(\mathbf{q},\omega)/\varepsilon(\mathbf{q},\omega)$, where ϕ_{ext} and ϕ_{tot} are the scalar potentials of the externally applied and the total electric fields, respectively. Since the cause is ϕ_{ext} and the effect is ϕ_{tot}, *not vice versa*, this is $1/\varepsilon$ that is guaranteed to be causal, but not ε itself [3]. Accordingly, KK relations must be satisfied by $1/\varepsilon$, but may or may not be satisfied by ε. For $|\mathbf{q}| > 0$, this leaves $\varepsilon(\mathbf{q},\omega = 0)$ a freedom to be negative without violating the causality or destroying the stability of the system [4,5]. If this happens, then the inverse permittivity has zeros in the upper half of the complex ω plane, making the permittivity itself a nonanalytic function.

In the three-dimensional (3D) world the realizations of such negative static permittivity are scarce and they mostly concern exotic noncrystalline systems [6–10]. In this Rapid Communication we show that, above a critical wave vector $q > q_c$ in the first Brillouin zone, the permittivity $\varepsilon(\mathbf{q},\omega)$ of quasi-two-dimensional (Q2D) systems of monolayer graphene and boron nitride is negative in the static limit. Accordingly, KK relations for the permittivity do not hold in this case. The inverse permittivity, on the contrary, remains causal and does satisfy KK relations.

We start by writing the permittivity of a Q2D crystal [11] (atomic units $e^2 = \hbar = m_e = 1$ are used throughout unless otherwise indicated),

$$\frac{1}{\epsilon(\mathbf{q},\omega)} = 1 + \frac{2\pi}{q}\int_{-\infty}^{\infty} \chi_{\mathbf{00}}(z,z',\mathbf{q},\omega)dzdz', \quad (1)$$

where $\chi_{\mathbf{GG}'}(z,z',\mathbf{q},\omega)$ is the density-response function of the system in the mixed, reciprocal in the system plane (xy), and real in the z-direction representation ($\mathbf{G}$ are the 2D reciprocal lattice vectors).

Our time-dependent density-functional theory (TDDFT) calculation of the permittivity consists of two steps. Since Q2D systems lack periodicity in the z direction, it is customary to use the supercell method [12–14]. First, in the supercell geometry, we calculate the density-response function $\tilde\chi_{\mathbf{G}g,\mathbf{G}'g'}(\mathbf{q},\omega;d)$ of an auxiliary 3D system comprising an infinite periodic array of monolayers with the separation d between them, as is schematized in Fig. 1(b) (the dependence of $\tilde\chi$ on d is shown explicitly). Here, g are reciprocal vectors in the z direction.

We have conducted the calculation for monolayer pristine graphene using the full-potential linear augmented plane-wave (FP-LAPW) code ELK [15]. The z-axis period d of the supercell was taken as 20 a.u. A k-point grid of $512 \times 512 \times 1$, 30 empty bands, and a damping parameter of 0.002 a.u. were used in both the ground-state and the linear-response calculations. The former was carried out within the local-density approximation (LDA) [16] for the exchange-correlation (xc) potential, while the latter was the random-phase approximation (RPA) one (i.e., the xc kernel f_{xc} [17] was set to zero).

Results for $\varepsilon_{3\text{D}}$, obtained through

$$\frac{1}{\varepsilon_{3\text{D}}(\mathbf{q},\omega;d)} = 1 + \frac{4\pi}{q^2}\tilde\chi_{\mathbf{0}0,\mathbf{0}0}(\mathbf{q},\omega;d), \quad (2)$$

are presented in the left panels of Figs. 2 and 3 for $q = 0.049$ and 0.152 a.u., respectively, along the ΓM direction.

It is, however, known that $\varepsilon_{3\text{D}}(\mathbf{q},\omega;d)$, calculated in the supercell geometry, is a quantity completely different from the permittivity $\varepsilon(\mathbf{q},\omega)$ of a single layer [11–14], as can be also immediately appreciated from the d dependence of the former. Our second step consists, therefore, in finding the density-response function χ of the single-layer system from that of the array of those layers $\tilde\chi$. This can be conveniently done by virtue of the matrix relation [11]

$$\chi(\mathbf{q},\omega) = \tilde\chi(\mathbf{q},\omega)[1 + C(\mathbf{q})\tilde\chi(\mathbf{q},\omega)]^{-1}, \quad (3)$$

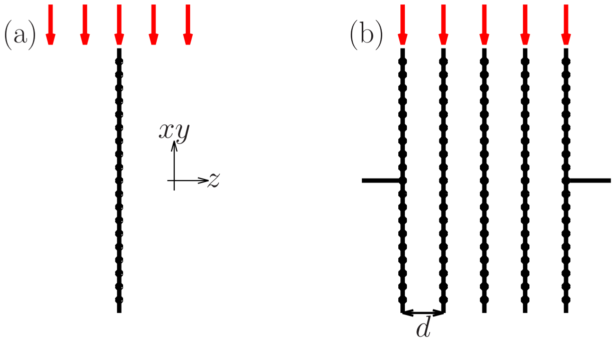

FIG. 1. (Color online) Schematics of 2D material under an external field. (a) Q2D single-layer geometry and (b) 3D supercell geometry.

where the elements of the matrix C are given by

$$C_{\mathbf{G}g,\mathbf{G}'g'}(\mathbf{q}) = F_{gg'}(|\mathbf{G}+\mathbf{q}|)\delta_{\mathbf{G}\mathbf{G}'},$$
$$F_{gg'}(p) = \frac{4\pi(p^2-gg')}{pd(p^2+g^2)(p^2+g'^2)} \times \cos\left[\frac{(g+g')d}{2}\right](1-e^{-pd}). \qquad (4)$$

In particular, χ calculated by Eqs. (3) and (4) is free of the spurious interlayer interaction, which is present in $\tilde{\chi}$.

By the use of Eqs. (3) and (4), we find χ in the 3D reciprocal-space representation. Then, by the inverse Fourier transform to the mixed representation and using Eq. (1), we obtain the permittivity $\varepsilon(\mathbf{q},\omega)$. The latter is plotted in the right panels of Figs. 2 and 3.

A striking feature in Fig. 3, right panel, is that $\varepsilon(\mathbf{q},\omega=0)$ is negative and, since $\mathrm{Im}\,\varepsilon(\mathbf{q},\omega \geqslant 0) \geqslant 0$, the permittivity of graphene does not satisfy the Kramers-Kronig relations [2]

$$\mathrm{Re}\,R(\omega) = R(\infty) + \frac{2}{\pi}\mathcal{P}\int_0^\infty \frac{\omega'\,\mathrm{Im}\,R(\omega')}{\omega'^2-\omega^2}d\omega',$$
$$\mathrm{Im}\,R(\omega) = -\frac{2\omega}{\pi}\mathcal{P}\int_0^\infty \frac{\mathrm{Re}\,R(\omega')-R(\infty)}{\omega'^2-\omega^2}d\omega', \qquad (5)$$

where $\mathcal{P}$ denotes the principal value of the integrals, with $R(\omega)=\varepsilon(\mathbf{q},\omega)$. This fact is further illustrated in Fig. 4, where the real part of $\varepsilon(\mathbf{q},\omega)$ is compared with the KK transform of its imaginary part: The two functions coincide at $q<q_c$ (left panel), but they are largely different at $q>q_c$ (right panel). We found the critical wave vector for graphene to be $q_c \approx 0.118$ a.u. (0.223 Å^{-1}) [18]. On the other hand, it can be seen in Figs. 2 and 3, left panels, that the array system has a positive static permittivity, which cannot be otherwise for a 3D periodic system within RPA [5].

Since the KK relations are not satisfied by $\varepsilon(\mathbf{q},\omega)$, the latter must have a singularity in the complex ω upper half plane. The

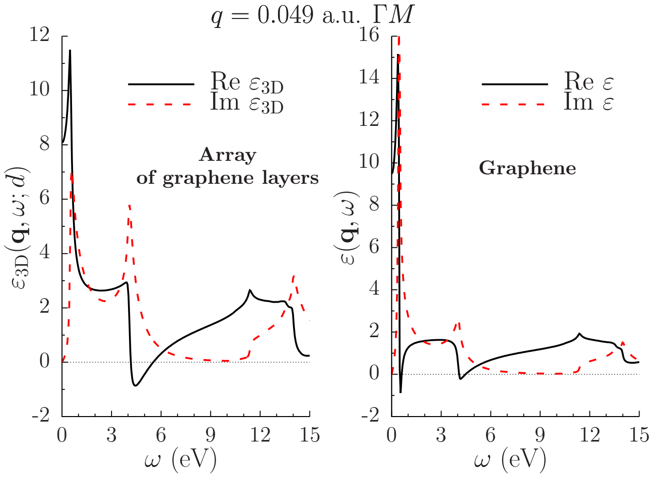

FIG. 2. (Color online) Left: 3D permittivity of the array of graphene layers. Right: Permittivity of a single graphene layer. The wave vector $q=0.049$ a.u. is below the critical value $q_c \approx 0.118$ a.u.

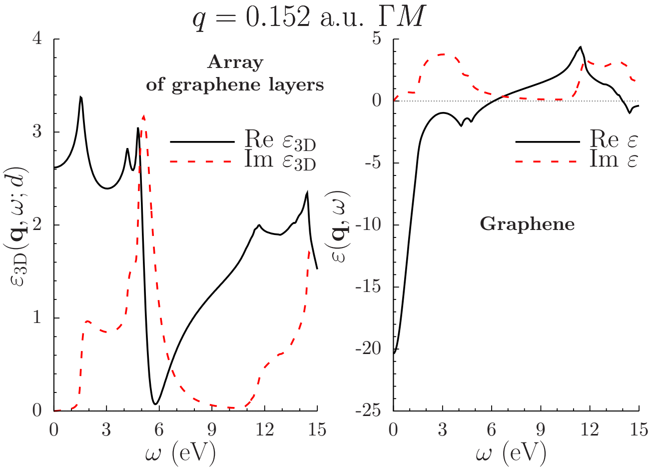

FIG. 3. (Color online) Left: 3D permittivity of the array of graphene layers. Right: Permittivity of a single graphene layer. The wave vector $q=0.152$ a.u. is above the critical value $q_c \approx 0.118$ a.u.

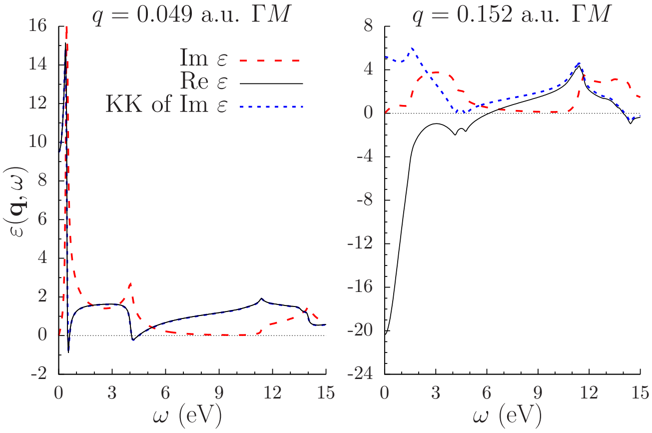

FIG. 4. (Color online) Real and imaginary parts of the permittivity of single-layer graphene. The real part obtained from the imaginary part by the use of the KK relation is plotted separately. Left: $q<q_c$, the KK relation holds. Right: $q>q_c$, the KK relation does not hold.

singularity can only be a pole at $\omega = \omega_s$, satisfying

$$\frac{1}{\varepsilon(\mathbf{q},\omega_s)} = 0. \tag{6}$$

Considering that (a) $1/\varepsilon(\mathbf{q},\omega)$ is a real continuous function on the positive imaginary axis of the ω plane, (b) $1/\varepsilon(\mathbf{q},\omega = 0) < 0$ for $q > q_c$, and (c) $1/\varepsilon(\mathbf{q},\omega = i\infty) = 1$, we conclude that, at $q > q_c$, there exists a point ω_s on the positive imaginary axis of the ω plane which satisfies Eq. (6). To find this point, we write, by virtue of Cauchy's integral formula,

$$\frac{1}{\varepsilon(\mathbf{q},iu)} - 1 = \frac{1}{2\pi i}\int_{-\infty}^{\infty} \frac{\frac{1}{\varepsilon(\mathbf{q},\omega')} - 1}{\omega' - iu} d\omega'. \tag{7}$$

Expanding the complex inverse permittivity in the right-hand side of Eq. (7) via its real and imaginary parts and using the parity properties of those functions, we can write

$$\frac{1}{\varepsilon(\mathbf{q},iu)} = 1 + \frac{1}{\pi}\int_0^{\infty} u\frac{\mathrm{Re}\frac{1}{\varepsilon(\mathbf{q},\omega')} - 1}{\omega'^2 + u^2} d\omega' + \frac{1}{\pi}\int_0^{\infty} \omega'\frac{\mathrm{Im}\frac{1}{\varepsilon(\mathbf{q},\omega')}}{\omega'^2 + u^2} d\omega'. \tag{8}$$

Further, the equality of the second term on the right-hand side to the third one can be easily proven with the use of the KK relations for $1/\varepsilon(\mathbf{q},\omega)$. We then have

$$\frac{1}{\varepsilon(\mathbf{q},iu)} = 1 + \frac{2}{\pi}\int_0^{\infty} \omega'\frac{\mathrm{Im}\frac{1}{\varepsilon(\mathbf{q},\omega')}}{\omega'^2 + u^2} d\omega'. \tag{9}$$

We use Eq. (9) to calculate the inverse permittivity on the positive imaginary ω axis from our results for it on the real axis. In Fig. 5, this is plotted for the two wave vectors, below and above the critical value.

Above the critical wave vector, the inverse permittivity crosses zero (indicated by a circle in Fig. 5), which does not happen below the critical wave vector. In Ref. [19], Sec. I, we compare our results with the analytical ones known in the low-q regime [20,21].

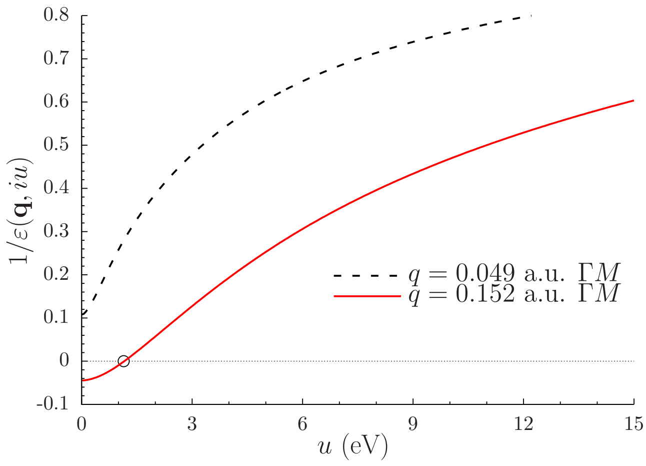

FIG. 5. (Color online) Inverse permittivity of a single graphene layer as a function of the imaginary frequency. At $q < q_c$ (black dashed curve), there is no zero (the permittivity is analytic in the upper complex ω plane). At $q > q_c$ (red solid curve), the inverse permittivity has a zero (indicated by a circle). Accordingly, the permittivity has a pole at this frequency.

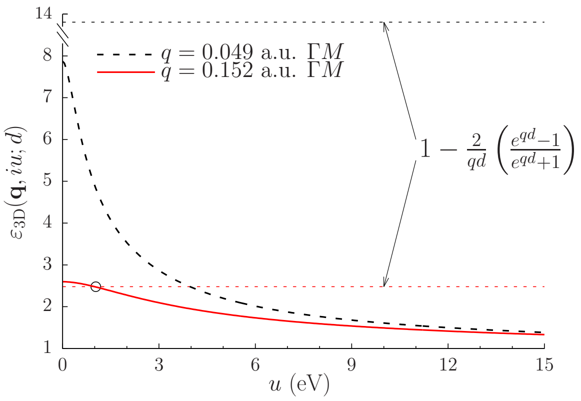

FIG. 6. (Color online) The permittivity of an array of graphene layers as a function of the imaginary frequency. The horizontal dashed lines show the values of $\varepsilon_{3\mathrm{D}}$ at which, by Eq. (11), the permittivity of single-layer graphene may become singular. This never happens at $q < q_c$ (black dashed curve), while this happens at $q > q_c$ (red solid curve).

We can gain further insight into the situation by using the approximate analytical relation between the Q2D permittivity of a single layer and the 3D permittivity of the array of those layers,

$$\frac{1}{\varepsilon(\mathbf{q},\omega)} = 1 + \frac{1}{2}\frac{1}{\frac{1}{\left[\frac{1}{\varepsilon_{3\mathrm{D}}(\mathbf{q},\omega;d)}-1\right]qd} + \frac{1}{e^{qd}-1}}, \tag{10}$$

rather than with the "exact" numerical solution of Eqs. (3) and (4). Equation (10), derived in Ref. [14], is a good approximation at q far from the critical value from both sides, as we demonstrate below in Fig. 7. Solving Eq. (10) with

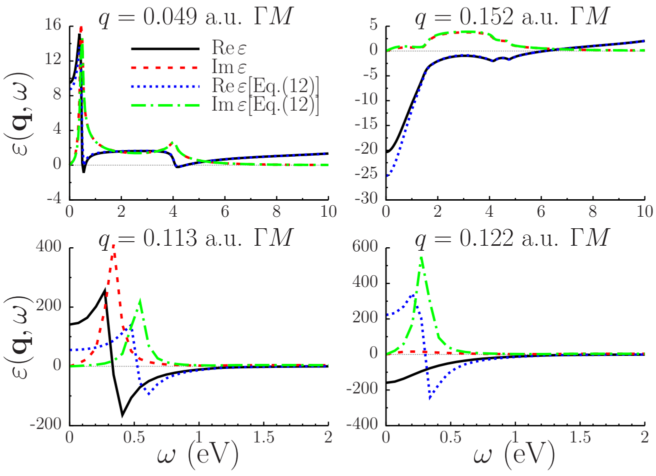

FIG. 7. (Color online) The permittivity of single-layer graphene calculated with the "exact" numerical procedure using Eqs. (3), (4), and (1), and the approximate analytical Eq. (10). Upper panels: The wave vector is *well* below (left) and above (right) the critical value $q_c \approx 0.118$ a.u. Lower panels: The wave vector is *slightly* below (left) and above (right) q_c.

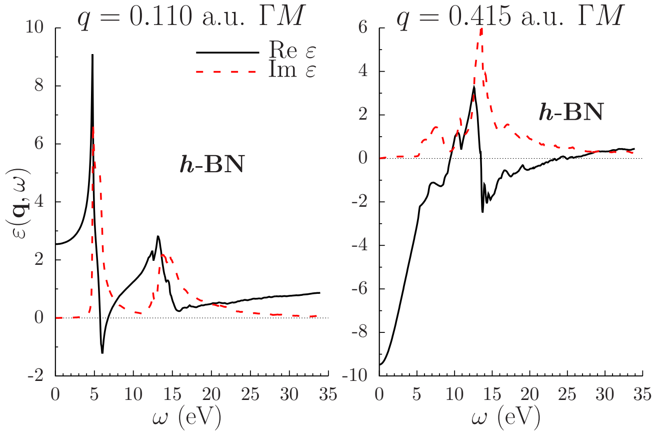

FIG. 8. (Color online) The permittivity of 2D hexagonal boron nitride below (left) and above (right) the critical wave vector $q_c \approx 0.323$ a.u.

respect to $\varepsilon_{3\mathrm{D}}$, we find that $1/\varepsilon$ is zero if

$$\varepsilon_{3\mathrm{D}}(\mathbf{q},\omega;d) = 1 - \frac{2}{qd}\left(\frac{e^{qd}-1}{e^{qd}+1}\right). \tag{11}$$

In Fig. 6, we plot $\varepsilon_{3\mathrm{D}}(\mathbf{q},\omega;d)$ along the positive imaginary ω. Although $\varepsilon_{3\mathrm{D}}(\mathbf{q},\omega;d)$ is analytic in the upper complex ω plane at all values of $\mathbf{q}$, it gives rise to a zero in $1/\varepsilon$ (a pole in ε) when condition (11) is met. In Fig. 6 this is shown as an intersection, in the case of $q > q_c$, with the straight horizontal line representing the right-hand side of Eq. (11).

Figure 7 is presented in support of the fact that the permittivity obtained through the "exact" numerical procedure via Eqs. (3), (4), and (1) can be accurately approximated by the simple analytical formula of Eq. (10), if q is sufficiently below or above the critical wave vector (upper panels). On the contrary, the same comparison done for the wave vector slightly below and above the critical value (lower panels) reveals the complete inapplicability of the approximate formula (10) in the vicinity of the critical wave vector. Moreover, a giant increase in the absolute value of the permittivity occurs close to the critical wave vector.

Graphene is known to be a semimetal, possessing a remarkable property of Dirac's cones touching in the K point of its band structure [22]. A natural question arises whether the negative static permittivity and the violation of KK relations in graphene are in any way related to the Dirac's cones in this material. To answer this, in Fig. 8 we present results for the permittivity of hexagonal boron nitride (*h*-BN), known to be an insulator [23]. Similar to graphene, above a critical wave vector $q_c \approx 0.323$ a.u. (0.610 Å^{-1}) (right panel of Fig. 8), the permittivity of BN does not satisfy the KK relations, while having a negative static limit. Furthermore, in Ref. [19], Sec. II, we demonstrate that a simple local model of a metallic slab in vacuum supports negative static permittivity at larger wave vectors. This shows that negative static permittivity and the breakdown of KK relations is a rather general property common to Q2D systems.

Importantly, in perfect 3D crystals, negative static permittivity is only possible due to the dynamic xc effects in the electronic response [5]. Since our results for Q2D crystals are obtained within the RPA, i.e., neglecting the xc effects, and the occurrence of negative static permittivity is possible, the situation is fundamentally different with Q2D crystals: This is the finite but microscopic thickness of the crystal, which is also the break of the periodicity in one dimension, that makes negative static permittivity possible. Nonetheless, static and dynamic many-body effects play an important part in Q2D crystals [24,25], which have not been accounted for in the present study. In Ref. [19], Sec. III, we show that the inclusion of the xc kernel f_{xc} on the level of the adiabatic time-dependent local-density approximation (ATDLDA) [17,26,27] does not lead to a significant change in the results. The inclusion of the same effects within TDDFT with more elaborate f_{xc}, e.g., following the schemes known in the 3D case [28,29], presents a challenge in the case of Q2D systems. Furthermore, for Q2D crystals supported on substrates, the interaction with the latter strongly influences the excitation processes [30], which is also a demanding problem to be addressed in the future.

For an accurate interpretation of the results, it is necessary to keep in mind the exact meaning of the permittivity (1) of a Q2D crystal. This definition is given in two steps [11]: First, the 2D conductivity $\sigma_{2\mathrm{D}}^{\mathrm{ext}}$ *with respect to the external field* is introduced,

$$\mathbf{j}_{2\mathrm{D}}(\mathbf{q},\omega) = \sigma_{2\mathrm{D}}^{\mathrm{ext}}(\mathbf{q},\omega)\mathbf{E}^{\mathrm{ext}}(\mathbf{q},\omega), \tag{12}$$

where $\mathbf{E}^{\mathrm{ext}}(\mathbf{q},\omega)$ is uniform in the z direction external electric field, and $\mathbf{j}_{2\mathrm{D}}(\mathbf{q},\omega)$ is the 3D current density *integrated in the z direction* and averaged over the unit cell in the xy plane. Second, the permittivity of a Q2D crystal is defined by the relation

$$\frac{1}{\varepsilon(\mathbf{q},\omega)} = 1 + \frac{2\pi q}{i\omega}\sigma_{2\mathrm{D}}^{\mathrm{ext}}(\mathbf{q},\omega), \tag{13}$$

rigorously valid for a strictly 2D system. The final justification of Eq. (13) is that, with this definition, the usual formula for the energy dissipation,

$$Q(\mathbf{q},\omega) = -\frac{\omega}{4\pi q}|\mathbf{E}_{\mathrm{ext}}(\mathbf{q},\omega)|^2\,\mathrm{Im}\frac{1}{\varepsilon(\mathbf{q},\omega),} \tag{14}$$

holds for a Q2D crystal exactly. However, as detailed in Ref. [11], the Q2D permittivity cannot be attributed the meaning of the coefficient of proportionality between the external and the total fields, and hence Eq. (14) cannot be rewritten in terms of $\mathbf{E}_{\mathrm{tot}}$ and $\mathrm{Im}\,\varepsilon$. We note that these complications call for particular caution in the consideration of negative static permittivity in the context of 2D superconductivity [4,5]. The behavior of the total field along the z direction in graphene is further discussed in Ref. [19], Sec. IV.

In conclusion, we have established the violation of Kramers-Kronig relations by the wave vector and frequency-dependent permittivity of quasi-two-dimensional graphene and boron nitride above a critical magnitude of the wave vector, and static permittivity was found to be negative in this case. The mechanism for negative static permittivity was shown to be conceptually different from that in the 3D case: It is due to the system finite microscopic thickness rather than to the exchange-correlation effects. Our findings suggest the fundamental differences between the screening and the electronic excitation processes in quasi-2D crystals as compared with both 3D and purely 2D systems. It is, however, discussed that further work is required to consider the present results in the context of 2D superconductivity.

I thank Guang-Yu Guo for valuable discussions. Support from the Ministry of Science and Technology, Taiwan, Grants No. 103-2112-M-001-007 and No. 104-2112-M-001-007, is acknowledged.

---

[1] D. Bohm, *Causality and Chance in Modern Physics* (Taylor and Francis, London, 2005).

[2] L. D. Landau and E. M. Lifshitz, *Electrodynamics of Continuous Media* (Pergamon, New York, 1960).

[3] D. Pines and P. Nozieres, *The Theory of Quantum Liquids* (Benjamin, New York, 1966).

[4] D. A. Kirzhnits, Sov. Phys. Usp. **19**, 530 (1976).

[5] O. V. Dolgov, D. A. Kirzhnits, and E. G. Maksimov, Rev. Mod. Phys. **53**, 81 (1981).

[6] J. P. Hansen and I. R. McDonald, Phys. Rev. Lett. **41**, 1379 (1978).

[7] A. Chandra and B. Bagchi, J. Chem. Phys. **91**, 3056 (1989).

[8] T. Fonseca and B. M. Ladanyi, J. Chem. Phys. **93**, 8148 (1990).

[9] M. Aniya, H. Okazaki, and M. Kobayashi, Phys. Rev. Lett. **65**, 1474 (1990).

[10] H. Yan, C. Zhao, K. Wang, L. Deng, M. Ma, and G. Xu, Appl. Phys. Lett. **102**, 062904 (2013).

[11] V. U. Nazarov, New J. Phys. **17**, 073018 (2015).

[12] C. A. Rozzi, D. Varsano, A. Marini, E. K. U. Gross, and A. Rubio, Phys. Rev. B **73**, 205119 (2006).

[13] V. Despoja, D. Novko, K. Dekanić, M. Šunjić, and L. Marušić, Phys. Rev. B **87**, 075447 (2013).

[14] V. U. Nazarov, F. Alharbi, T. S. Fisher, and S. Kais, Phys. Rev. B **89**, 195423 (2014).

[15] http://elk.sourceforge.net.

[16] J. P. Perdew and Y. Wang, Phys. Rev. B **45**, 13244 (1992).

[17] E. K. U. Gross and W. Kohn, Phys. Rev. Lett. **55**, 2850 (1985).

[18] Generally speaking, q_c is different in different directions, however, it is practically isotropic in graphene.

[19] See Supplemental Material at http://link.aps.org/supplemental/10.1103/PhysRevB.92.161402 for (i) low-q limit of the permittivity of graphene, (ii) slab model, with an illustration of the negative static permittivity of a Q2D system, (iii) results of calculations within ATDLDA, and (iv) plots of the distribution of the charge density and the potential.

[20] J. F. Dobson, A. White, and A. Rubio, Phys. Rev. Lett. **96**, 073201 (2006).

[21] B. Wunsch, T. Stauber, F. Sols, and F. Guinea, New J. Phys. **8**, 318 (2006).

[22] A. H. Castro Neto, F. Guinea, N. M. R. Peres, K. S. Novoselov, and A. K. Geim, Rev. Mod. Phys. **81**, 109 (2009).

[23] Y. Lin and J. W. Connell, Nanoscale **4**, 6908 (2012).

[24] L. Yang, J. Deslippe, C.-H. Park, M. L. Cohen, and S. G. Louie, Phys. Rev. Lett. **103**, 186802 (2009).

[25] V. N. Kotov, B. Uchoa, V. M. Pereira, F. Guinea, and A. H. Castro Neto, Rev. Mod. Phys. **84**, 1067 (2012).

[26] A. Zangwill and P. Soven, Phys. Rev. A **21**, 1561 (1980).

[27] E. Runge and E. K. U. Gross, Phys. Rev. Lett. **52**, 997 (1984).

[28] S. Botti, F. Sottile, N. Vast, V. Olevano, L. Reining, H.-C. Weissker, A. Rubio, G. Onida, R. Del Sole, and R. W. Godby, Phys. Rev. B **69**, 155112 (2004).

[29] V. U. Nazarov and G. Vignale, Phys. Rev. Lett. **107**, 216402 (2011).

[30] A. Politano and G. Chiarello, Nanoscale **6**, 10927 (2014).